

Quantitative phase analysis of strongly textured alloy mixtures using neutron diffraction

E. J. Shin,^a B. S. Seong,^b C. H. Lee^b and M. Y. Huh^{a*}

Received 9 January 2002

Accepted 11 June 2002

^aDivision of Materials Science and Engineering, Korea University, Seoul, 136-701, Korea, and^bHANARO Center, Korea Atomic Energy Research Institute, Taejeon 305-600, PO Box 105, Korea.

Correspondence e-mail: myhuh@korea.ac.kr

Based on the Rietveld profile refinement of neutron diffraction patterns and a new texture analysis method, a quantitative phase analysis (QPA) method is proposed and examined in the case of artificially produced multiphase alloys having strong textures. The preferred-orientation factors (POFs) of the diffraction peaks were extracted from the inverse pole figure calculated from the orientation distribution function (ODF) that was computed from the averaged pole figures measured by the rotating sample stage, providing a faster and simpler texture measurement. The reliability of this method was examined using binary alloy mixtures of known fractions of zirconium and aluminium. In addition, the fraction of unknown phases in an artificially produced aluminium matrix composite was determined by introducing a standard zirconium sample. QPA of the binary mixtures successfully predicted the weight fraction of each component with an absolute error of less than 0.3 wt%. This method also provided appropriate results on the calculation of the weight fraction of unknown phases in the aluminium matrix composite.

© 2002 International Union of Crystallography
Printed in Great Britain – all rights reserved

1. Introduction

The methods of determining the amount of each phase in an multiphase alloy, *i.e.* quantitative phase analysis (QPA), involve the observation of microstructures, Mössbauer spectroscopy (Fysh & Lee, 1985; Ma *et al.*, 1989), a magnetic technique (Hilliard & Cahn, 1961), X-ray (Averbach *et al.*, 1959; Arnell & Ridal, 1968) and neutron diffraction, *etc.* Among these methods, QPA using X-ray diffraction data has prevailed for decades since it provides results for powder samples. Because powder samples are homogenous, analytic errors from inhomogeneous distributions of grain orientations and phases throughout the sample can be generally neglected. However, grain orientations and phases in most commercial alloys, whether naturally occurring or fabricated, are rarely randomly distributed. Accordingly, the conventional X-ray diffraction techniques that rely on the comparison of the intensities of particular diffraction peaks often mislead the QPA of commercial alloys having textures (preferred orientations) and second or third phases. In contrast to conventional X-ray diffraction techniques, the whole-pattern fitting method, utilizing a large number of diffraction peaks and the strong penetrating power of the neutron, enable a more precise QPA of polycrystalline materials (Bacon, 1975; Hill & Howard, 1987).

The Rietveld method, one of the whole-pattern fitting methods, is a powerful tool for the determination of crystalline structures, as well as for QPA of powder samples (Hill & Howard, 1987; Bish & Howard, 1988). As it uses the entire diffraction pattern, Rietveld refinement offers the advantage

of accurate calculations in the case of patterns with weak intensity owing to the small amount of sample. Furthermore, neutron diffraction patterns enable more accurate QPA calculations because neutron diffraction data represent the bulk sample. However, a proper correction is required in the case of the Rietveld refinement of highly textured samples. The March–Dollase function (Dollase, 1986; Howard & Kisi, 2000) is basically used for the correction of preferred orientation, but its application to highly textured samples (*e.g.* rolled sheets) is generally limited (Kim *et al.*, 2001).

With regard to texture effects in Rietveld refinement, a number of successful works have been reported, combining quantitative texture analysis with the Rietveld method for profile refinement. Choi *et al.* (1994) calculated the orientation distribution function (ODF) by measuring a few complete pole figures and extracted the preferred-orientation factors (POFs) by means of calculated inverse pole figures. The POFs were then used to improve the Rietveld refinement of diffraction patterns measured by a θ – 2θ scan with a single detector. On the other hand, Lutterotti *et al.* (1997), Matthies *et al.* (1997) and Von Dreele (1997) determined the ODF from dozens of diffraction patterns pertaining to a variety of sample orientations. However, the methods mentioned above require a long measuring time. Recently, Kim *et al.* (2001) reported a less time-consuming method, involving the measurement of neutron diffraction patterns with a multiple-detector and introducing the procedure of extracting the POFs from a number of pole figures, recalculated from the ODF that was calculated from several measured complete pole figures. In

Table 1

The QPA results of the binary mixtures consisting of aluminium and zirconium.

Numbers in parentheses are the standard deviations resulting from Rietveld fitting.

Sample	As weighed (wt%)		Results of refinement					
			With correction†		Without correction‡		March– Dollase§	
			χ^2	wt%	χ^2	wt%	χ^2	wt%
ZA1	Zr	75.71	3.6	75.50 (0.62)	75.6	76.93 (3.28)	18.9	83.88 (2.90)
	Al	24.29		24.50 (0.25)		23.07 (1.81)		16.12 (1.66)
ZA2	Zr	85.89	4.9	85.82 (0.66)	116	86.29 (3.43)	27.6	89.92 (2.20)
	Al	14.11		14.18 (0.16)		13.71 (1.38)		10.08 (0.77)
ZA3	Zr	90.62	4.8	90.71 (0.74)	113	91.26 (3.61)	26.9	94.07 (2.28)
	Al	9.38		9.29 (0.25)		8.74 (1.18)		5.93 (0.60)
ZA4	Zr	95.90	5.9	95.90 (0.78)	111	95.02 (3.57)	26.6	96.56 (2.31)
	Al	4.10		4.10 (0.19)		4.98 (1.07)		3.44 (0.56)

† Rietveld fits with the preferred orientation correction using POFs. ‡ Rietveld fits without a preferred orientation correction. § Rietveld fits with the preferred orientation correction using a March–Dollase function.

Table 2

The QPA results of the artificial aluminium matrix composite containing copper as the unknown phase.

The weight of zirconium as a standard sample is 1.89 g. The final column gives the absolute error in wt% of Cu.

Sample	As weighed			Results of refinement		Calculated		Error (wt%)
	Al (g)	Cu (g)	Cu (wt%)	χ^2	Zr (wt%)	Cu (g)	Cu (wt%)	
ZAC1	2.65	0.19	6.69	11.7	41.64	0.19	6.69	0.00
ZAC2		0.29	9.86	18.0	41.55	0.28	9.52	-0.34
ZAC3		0.40	13.11	23.7	41.79	0.41	13.44	-0.33
ZAC4		0.50	15.87	30.5	41.70	0.51	16.19	-0.32
ZAC5		0.80	23.19	49.9	41.64	0.81	23.48	-0.29

this method, all the $\{hkl\}$ pole figures should be calculated in order to determine the POF of the corresponding individual scattering-vector direction $2\theta_{hkl}$.

In line with previous research by Choi *et al.* (1994) and Kim *et al.* (2001), we propose a new method for preferred-orientation correction and apply this method to the Rietveld QPA approach. In contrast to the previous work, the POFs of diffraction peaks were extracted from the inverse pole figure calculated from the ODF that was calculated from the averaged pole figures measured by the rotating sample stage, providing a faster and simpler texture measurement. The reliability of this method was examined using binary mixtures of known fractions of zirconium and aluminium. Fractions of unknown phases in artificially produced aluminium matrix composites were also determined by introducing a standard zirconium sample.

2. Experimental procedure

As-received materials were hot-rolled strips of zirconium, aluminium and copper with purities of 99.7, 99.9 and 99%, respectively. In order to obtain a strong texture, the aluminium

hot-rolled strip was first cold rolled to 90% thickness reduction and then recrystallized at 573 K for 1 h. A series of binary mixtures of zirconium–aluminium and another series of ternary mixtures of zirconium–aluminium–copper were prepared by stacking small plates cut from sheets. The compositions of the mixtures are listed in Tables 1 and 2. Cube-shaped specimens, about $10 \times 10 \times 10$ mm, were examined for the measurement of texture.

The crystallographic textures were determined by measuring complete pole figures by means of the four-circle diffractometer (FCD), using a neutron beam of wavelength 0.99 \AA , at the HANARO reactor of the Korea Atomic Energy Research Institute. Six and three complete pole figures were measured for zirconium and aluminium, respectively. First, the texture was determined by the usual complete pole figure. In this procedure, the pole figures were scanned on both the radial angle α and the azimuth angle β , with a constant interval of 5° . For a complete pole figure, the pole density P_{hkl} of $(\alpha \times \beta) = 19 \times 72$ points was measured.

In addition to the usual method, a new method of texture determination was introduced by the installation of a rotating (~ 60 r.p.m.) sample stage on the FCD. By means of this method, the pole density P_{hkl} of the $\{hkl\}$ pole figure was measured only along the radial angle α , because the rotation of the sample provided an average value of $P_{hkl}(\alpha, \beta)$ with a constant α and varying azimuth angle β :

$$P_{hkl}(\alpha) = \pi \oint P_{hkl}(\alpha, \beta) d\beta. \quad (1)$$

Accordingly, $P_{hkl}(\alpha)$ was measured for only 19 points for a construction of a complete pole figure ($\alpha = 0 \sim 90^\circ$, $\Delta\alpha = 5^\circ$). From these averaged complete pole figures, ODFs were calculated by the WIMV (Williams–Imhof–Matthies–Vinel) (Matthies & Vinel, 1982) program of the software package BEARTEX (Wenk & Matthies, 1999).

Diffraction patterns were measured with the high-resolution powder diffractometer (HRPD), equipped with 32 detectors ($\Delta d/d \simeq 2.0 \times 10^{-3}$), at the HANARO reactor. A neutron beam of wavelength 1.84 \AA was used. The data were collected at intervals of 0.05° between 10 and 155° in 2θ , with sample rotation of about 30 r.p.m.; the normal direction (ND) of the sample was parallel to the rotation axis and a set of detectors were placed in the plane perpendicular to the rotating axis. The program FULLPROF (Rodriguez-Carvajal, 1998) was used for the Rietveld refinement calculations.

3. Rietveld profile refinement and extraction of POF values

In angle-dispersive neutron (or X-ray) diffraction, the intensity at a point i of a multiphased polycrystalline material may be expressed by (Rietveld, 1969; Choi *et al.*, 1994)

$$Y_i = \sum_j \sum_k [s_j L_{jk} J_{jk} P_{jk} |F_{jk}|^2 \varphi(2\theta_i - 2\theta_{jk})] a_i + b_i, \quad (2)$$

where the subscripts are i for the scattering angles, j for the j th phase, and k for the k th reflection plane of each phase. The parameters s_j , L_{jk} , J_{jk} , P_{jk} , F_{jk} and φ are the scale factor, the

Lorentz factor, the multiplicity, the POF, the structure factor and the profile function of the k th peak of the j th phase, respectively. a_i and b_i are the absorption factor and the background intensity at the i th scattering position, respectively.

The POFs P_{jk} can be extracted from the pole density distribution as the result of the texture analysis (Choi *et al.*, 1994; Kim *et al.*, 2001). In this work, the POFs were extracted from the inverse pole figures of the radial direction ($\alpha = \pi/2$) calculated from the ODFs, which were computed from the averaged complete pole figures. The radial direction is one of the sample directions perpendicular to the ND. Note that during the measurements of the texture as well as the diffraction pattern, samples were rotated around the ND. As mentioned in §2, during the measurement of diffraction patterns a set of detectors were placed in the plane perpendicular to the rotating axis of the sample. Therefore, rotational symmetry about the axis (fibre texture) exists and the sample direction of the diffraction peaks corresponds to $\alpha = \pi/2$ in the pole figure.

The scale factor of the j th phase can be written (Hill & Howard, 1987)

$$s_j \propto m_j / (Z_j M_j V_j), \quad (3)$$

where m , Z , M and V are the mass of the j th phase, the number of formula units per unit cell, the mass per formula unit and the unit-cell volume, respectively. The weight fraction f of each phase can be determined from the four parameters (s , Z , M and V) for all phases by

$$f_j = (s_j Z_j M_j V_j) / \sum_i (s_i Z_i M_i V_i). \quad (4)$$

The QPA is based on equation (4).

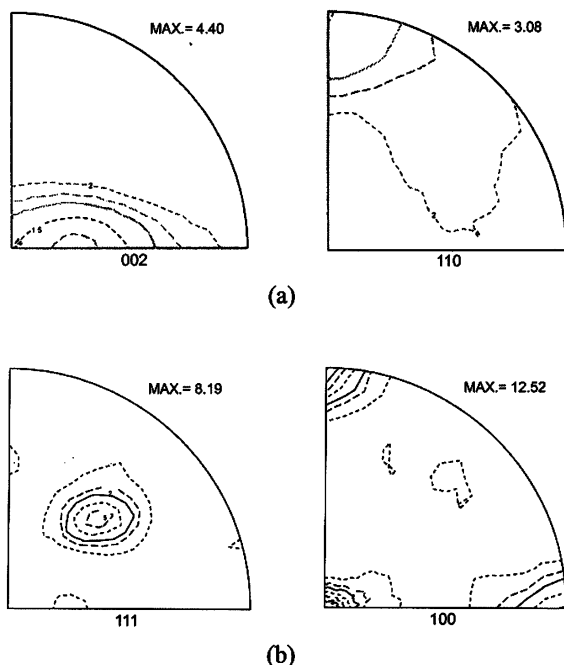


Figure 1
Normalized experimental complete pole figures: (a) zirconium; (b) aluminium.

4. Results and discussion

4.1. Evaluation of textures and POFs

In order to verify the reliability of the texture determination using the rotating sample stage, the texture of zirconium and aluminium sheets was determined by the usual complete pole figure. Some examples of usual normalized complete pole figures are shown in Fig. 1.

The texture of the zirconium hot-rolled strip in Fig. 1(a) can be characterized by the $\{110\}$ and $\{002\}$ pole figures. The zirconium sample exhibited $\langle 110 \rangle \parallel \text{RD}$ preferred orientations with the basal plane $\{002\}$ lying 20° away from the ND. $\langle 110 \rangle \parallel \text{RD}$ denotes a fibre texture comprising orientations with a common $\langle 110 \rangle$ direction parallel to the rolling direction. The maximum pole density $P_{002}^{\text{max}} = 4.40$ was obtained in the $\{002\}$ pole figure of the zirconium sample. The ODFs calculated from the set of three complete pole figures provided the maximum orientation density $f(g)^{\text{max}} = 5.8$.

Fig. 1(b) shows the $\{111\}$ and $\{200\}$ pole figures of the aluminium sample. The cold rolling to 90% thickness reduction and the subsequent recrystallization anneal of aluminium led to a texture that was dominated by a strong cubic orientation $\{001\}\langle 100 \rangle$ (Humphreys & Hetherly, 1995). For the aluminium sample, $P_{200}^{\text{max}} = 12.52$ was obtained and $f(g)^{\text{max}} = 63.1$ was calculated. A large value of $f(g)^{\text{max}}$ is attributed to the symmetry of the cubic crystal system.

It was noted that the pole figures measured for the pure samples and for the mixtures were identical. This result is attributed to the well isolated diffraction peaks obtained for the test mixtures of zirconium and aluminium.

The texture was obtained next with the rotating sample stage. After measuring the pole density $P_{hkl}(\alpha)$, a complete

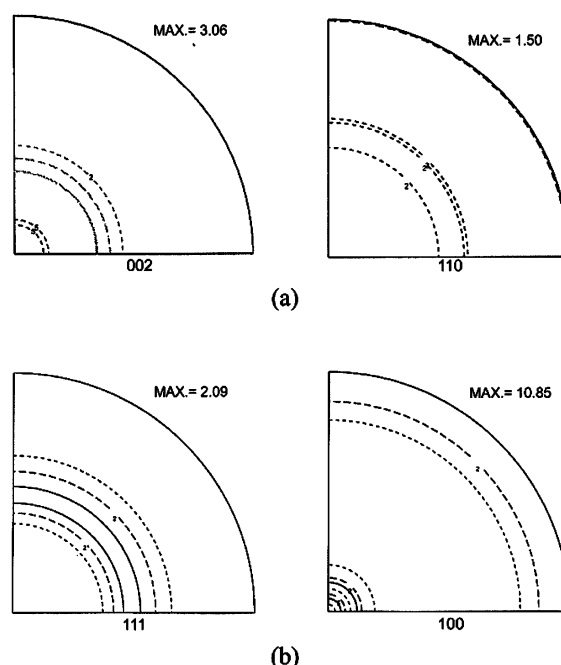


Figure 2
Normalized experimental averaged pole figures measured by rotating the sample stage: (a) zirconium; (b) aluminium.

pole figure was constructed by taking $P_{hkl}(\alpha)$ as the $P_{hkl}(\alpha, \beta)$ (Fig. 2). The maximum pole densities of zirconium and aluminium are $P_{002}^{\max} = 3.06$ and $P_{200}^{\max} = 10.85$, respectively. The pole figures of the rotated sample can also be obtained mathematically by averaging the $P_{hkl}(\alpha, \beta)$ along the same α direction as for the usual pole figures, as shown in Fig. 1. From complete pole figures of the rotated samples, ODFs were computed. The inverse pole figure of a radial direction ($\alpha = \pi/2$) was calculated from these ODFs. Fig. 3 shows the inverse pole figures obtained from the averaged pole figures of the zirconium and aluminium samples. Owing to the different crystal systems, the symmetrically equivalent space of the crystal coordinate system and the crystallographic direction indices are defined differently for zirconium and aluminium. The crystallographic directions close to $\langle uv0 \rangle$ have a high value of P_{uvw} for the zirconium sample, whereas the maximum P_{uvw} is found in the direction of $\langle 100 \rangle$ in the case of aluminium. The P_{uvw} shown in Fig. 3 is equivalent to the POF of the $\langle uvw \rangle$ crystal direction.

4.2. QPA of binary mixtures

As an example of the QPA, the neutron diffraction pattern of a binary mixture (sample ZA4) comprising the zirconium and aluminium sheet is displayed with the Rietveld fit in Fig. 4. The binary mixture contains 4.10 wt% of aluminium. In Fig. 4(a), the experimental pattern is shown with the Rietveld fit performed under the assumption of a randomly textured sample. It is obvious that this assumption gives rise to a bad fit. Fig. 4(b) shows the same diffraction pattern and the Rietveld fit calculated together with the texture correction. Apparently, a good fit is obtained by taking account of the POFs extracted from the inverse pole figures of Fig. 3.

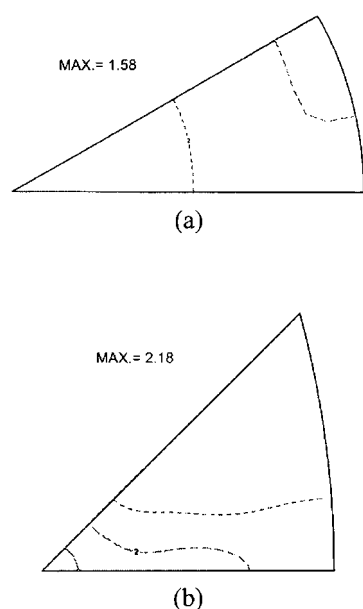


Figure 3 Inverse pole figures calculated from the averaged pole figures: (a) zirconium; (b) aluminium.

In order to examine the reliability of the present QPA method, four binary mixtures (ZA1 to ZA4) comprising the zirconium and aluminium sheets were prepared. QPA results and the values of the criteria of fit, χ^2 , of each phase are listed in Table 1. QPA results were determined from three different Rietveld fits with and without preferred-orientation correction, and also with a March–Dollase correction. The correctness of the QPA can be estimated by comparing the weight fraction of components weighed practically with that obtained from the QPA. It turns out that the application of the present method to a strongly textured binary mixture provides a fairly convincing QPA with an absolute error of less than -0.21 wt%. The goodness of fit, χ^2 , was less than 5.9 for all binary mixtures.

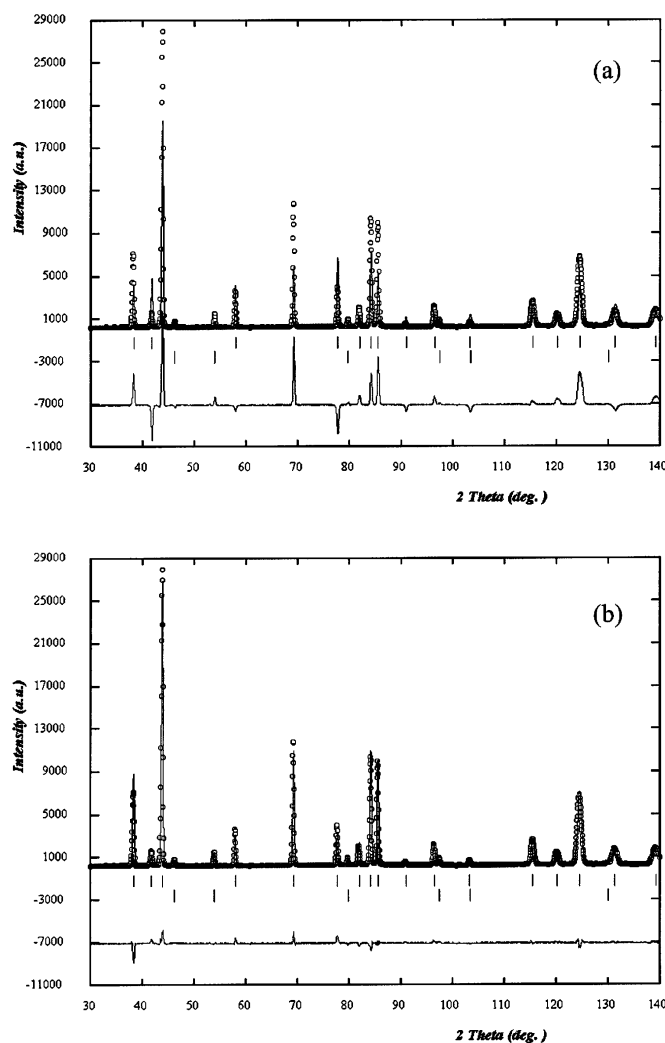


Figure 4 Diffraction patterns of the ZA4 sample measured in 2θ scan mode: (a) without the correction for preferred orientation and (b) with the correction for preferred orientation. Circles are the observed intensities and the upper solid line represents the calculated fit. The lower solid line represents the difference. The two rows of small bars represent the Bragg reflection positions of zirconium (upper) and aluminium (lower).

4.3. QPA of the aluminium matrix composite containing unknown phase

Most polycrystalline metals and alloys exhibit texture and also contain foreign phases of precipitates or inclusions in their matrix phase. Commercial aluminium alloy sheets are typical examples. For QPA results to be reliable, the number of overlapped diffraction peaks from mixed phases should be minimal. This is generally true in the case of intermetallic precipitates formed in most aluminium alloys. In order to assess the application of the present QPA method to aluminium alloys, several mixtures, *i.e.* artificial aluminium matrix composites comprising aluminium and copper, were prepared. In the samples, aluminium and copper were assumed as the aluminium matrix and unknown phase, respectively.

For the QPA, a standard sample of the zirconium hot band was adapted, because most diffraction peaks from zirconium are not overlapped with those of aluminium. The weight of the composite, W_{comp} , and the standard sample, W_{Zr} , were determined experimentally. With known W_{comp} and W_{Zr} , the sample for the measurement of neutron diffraction patterns was prepared by stacking the composite together with the standard sample. Under the assumption that the diffraction peaks of zirconium and aluminium are not affected by the unknown phase in the composite, the weight fraction of zirconium, f_{Zr} , and aluminium, f_{Al} , can be determined by the QPA described above. Now, the weight W_{up} of the unknown phase is simply obtained by

$$W_{\text{up}} = W_{\text{comp}} + W_{\text{Zr}} - W_{\text{Zr}}/f_{\text{Zr}}. \quad (5)$$

The neutron diffraction pattern of the sample comprising the composite (sample ZAC1, $W_{\text{Cu}} = 0.19$ g) and the standard sample is displayed with the Rietveld fit in Fig. 5. As readily seen from the difference plot (lower solid line), the difference between the experimentally measured and the calculated

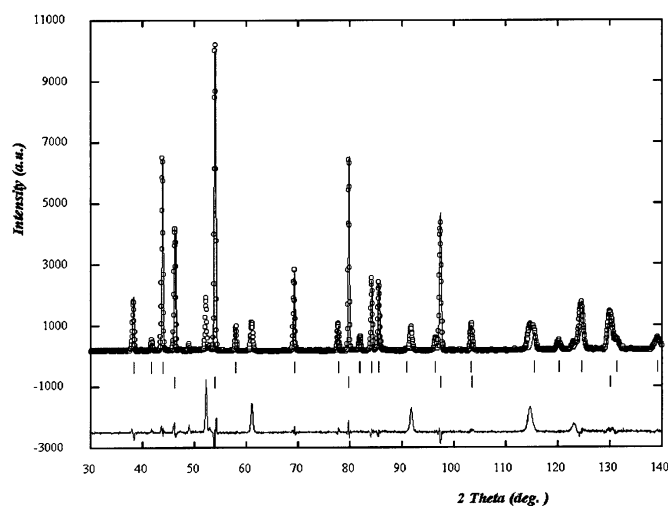


Figure 5 Diffraction patterns of the ZAC1 sample measured in 2θ scan mode: circles are the observed intensities and the upper solid line represents the calculated fit. The lower solid line represents the difference. The two rows of small bars represent the Bragg reflection positions of zirconium (upper) and aluminium (lower).

pattern is not large at the peak positions of zirconium and aluminium. While the sample comprised copper as an unknown phase, the Rietveld fit was performed under the assumption of a binary system of zirconium and aluminium. Accordingly, it is obvious that the large difference of the lower solid line is found at the peak positions of copper. The QPA results for five artificial composite samples containing copper of $W_{\text{Cu}} = 0.19\sim 0.80$ g are listed in Table 2. The weight fraction of copper was successfully calculated within a 0.34 wt% error band. The value of the goodness of fit, χ^2 , gradually increases with increasing copper content in the composite, owing to neglecting the content of copper in the calculation of the Rietveld profile. However, values of χ^2 for the whole pattern of the composite and the standard sample are not very meaningful for the QPA of the unknown phase because only the calculation of the Rietveld fit on peaks of aluminium and zirconium is required in the QPA procedure proposed in this work.

5. Conclusions

A new preferred-orientation correction method is proposed and has been applied to QPA based on Rietveld profile refinement. The POFs of diffraction peaks were extracted from the inverse pole figure calculated from the ODF that was calculated from the averaged pole figures measured by the rotating sample stage, providing a faster and simpler texture measurement. Applying this method to binary mixtures of known fractions of strongly textured zirconium and aluminium gave rise to a fairly convincing QPA with an error of less than -0.21 wt%. The goodness of fit χ^2 was less than 5.9 for all binary mixtures. By introducing a standard zirconium sample, the weight fraction of unknown phases in the artificially produced aluminium matrix composite was successfully calculated with an error of less than -0.34 wt%. Accordingly, it is verified that the QPA procedure proposed in this work is applicable to determine the weight fraction of phases in multi-phase systems having strong textures.

The authors are grateful to Dr Y. C. Kim for valuable discussions. This work has been carried out under the Nuclear R&D Program of the Ministry of Science and Technology.

References

- Arnell, R. D. & Ridal, K. A. (1968). *J. Iron Steel Inst.* **206**, 1035–1036.
- Averbach, B. L., Comerford, M. F. & Bever, M. B. (1959). *Trans. AIME*, **215**, 682–685.
- Bacon, G. E. (1975). *Neutron Diffraction*. Oxford: Clarendon Press.
- Bish, D. L. & Howard, S. A. (1988). *J. Appl. Cryst.* **21**, 86–91.
- Choi, C. S., Baker, E. F. & Orosz, J. (1994). *Adv. X-ray Anal.* **37**, 49–57.
- Dollase, W. A. (1986). *J. Appl. Cryst.* **19**, 267–272.
- Fysh, S. A. & Lee, J. B. (1985). *Proceedings of the 5th Process Technical Conference: Measurement and Control Instrumentation in the Iron and Steel Industry, Detroit, MI, USA*, pp. 4–17. ISS-AIME.
- Hill, R. J. & Howard, C. J. (1987). *J. Appl. Cryst.* **20**, 467–474.
- Hilliard, J. E. & Cahn, J. W. (1961). *Trans. AIME*, **221**, 344–352.
- Howard, C. J. & Kisi, E. H. (2000). *J. Appl. Cryst.* **33**, 1434–1435.

- Humphreys, F. J. & Hetherly, M. (1995). *Recrystallization and Related Phenomena*. Oxford: Elsevier Science.
- Kim, Y. C., Seong, B. S., Lee, J. H. & Shin, E. J. (2001). *J. Appl. Cryst.* **34**, 358–364.
- Lutterotti, L., Matthies, S., Wenk, H.-R., Schultz, A. S. & Richardson, J. W. (1997). *J. Appl. Phys.* **81**, 594–600.
- Ma, R., Zhang, H., Shu, S., Chang, R., Jin, H. & Xu, G. (1989). *Trans. Met. Heat Treat.* **10**, 54–58.
- Matthies, S., Lutterotti, L. & Wenk, H.-R. (1997). *J. Appl. Cryst.* **30**, 31–42.
- Matthies, S. & Vinel, G. (1982). *Phys. Status Solidi B*, **112**, K111–K120.
- Rietveld, H. M. (1969). *J. Appl. Cryst.* **2**, 65–71.
- Rodriguez-Carvajal, J. (1998). *FULLPROF*, Version 3.5d. Laboratoire Leon Brillouin, Saclay, France.
- Shin, E. J., Seong, B. S., Lee, C. H. & Huh, M. Y. (2001). *J. Phys. Soc. Jpn*, **70**(suppl.), 542–544.
- Von Dreele, R. B. (1997). *J. Appl. Cryst.* **30**, 517–525.
- Wenk, H.-R. & Matthies, S. (1999). *BEARTEX*, Berkeley Texture Package, Version 1.1. Berkeley, USA.